Heterogeneous & Homogeneous & Bio- & Nano-
CHEMCATCHEM
CATALYSIS

Accepted Article

Title: Selective C-C Hydrogenolysis of Alkylbenzenes to Methylbenzenes with Suppression of Ring Hydrogenation

Authors: Shin Yanatake, Yosuke Nakaji, Mii Betchaku, Yoshinao Nakagawa, Masazumi Tamura, and Keiichi Tomishige

To be cited as: *ChemCatChem* 10.1002/cctc.201801118

Link to VoR: http://dx.doi.org/10.1002/cctc.201801118

A Journal of ChemPubSoc Europe

WILEY-VCH www.chemcatchem.org

Selective C-C Hydrogenolysis of Alkylbenzenes to Methylbenzenes with Suppression of Ring Hydrogenation

Shin Yanatake,[a] Yosuke Nakaji,[a] Mii Betchaku,[a] Yoshinao Nakagawa,[a,b,*] Masazumi Tamura[a,b] and Keiichi Tomishige[a,b,*]

[a]

Shin Yanatake, Yosuke Nakaji, Mii Betchaku, Dr. Yoshinao Nakagawa, Dr. Masazumi Tamura, Prof. Dr. Keiichi Tomishige

Department of Applied Chemistry, School of Engineering, Tohoku University, 6-6-07 Aoba, Aramaki, Aoba-ku, Sendai, 980-8579, Japan

[b]

Dr. Yoshinao Nakagawa, Dr. Masazumi Tamura, Prof. Dr. Keiichi Tomishige

Research Center for Rare Metal and Green Innovation, Tohoku University, 468-1, Aoba, Aramaki, Aoba-ku, Sendai 980-0845, Japan

* Corresponding authors.

E-mail: yoshinao@erec.che.tohoku.ac.jp, Tel/Fax: +81-22-795-7215 (Y. N.);

tomi@erec.che.tohoku.ac.jp, Tel&Fax: +81-22-795-7214 (K. T.)

Abstract

Selective reduction of alkylbenzenes, which are supplied by refining heavy hydrocarbons, to methylbenzenes by selective C-C hydrogenolysis was accomplished by Ru/CeO_2 catalyst. Hydrogenolysis of ethylbenzene was carried out with gas-phase fixed-bed flow reactor and various noble metal catalysts. The catalyst with high Ru loading (4 wt%) on CeO_2 support pre-calcined at high temperature (1073 K; $Ru(4)/CeO_2^{1073}$ catalyst) showed both good activity and selectivity to toluene. The yield of toluene reached 65 %-C in the conditions of 533 K and H_2 partial pressure of 0.075 MPa. Hydrogenolysis of other alkylbenzenes including *p*-ethyltoluene, propylbenzene and cumene was also carried out. Hydrogenolysis of C_{aryl}-C_{alkyl} bond and hydrogenation of benzene ring was slow in all substrate cases. Hydrogenolysis of *p*-ethyltoluene can give *p*-xylene as the main product (highest yield: 53 %-C). These high yields of methylbenzenes make a marked contrast to the traditional bifunctional hydrocracking systems which preferably dissociate C_{aryl}-C_{alkyl} bond in alkylbenzenes. Characterization of Ru catalysts suggests that the block-shaped Ru particles with small size (<2 nm) in $Ru(4)/CeO_2^{1073}$ give good catalytic performance. Too strong interaction between Ru species and CeO_2 support induced by decreasing the loading amount rather gives ring-hydrogenation activity and decreases methylbenzenes selectivity.

Keywords

Heterogeneous catalysis, Cleavage reactions, BTX, Ruthenium, ceria support

1. Introduction

Conversions of heavy hydrocarbon resources into value-added chemicals are becoming more and more important, since heavier crude oil with high mining cost has been more supplied.[1] Monoaromatic hydrocarbons with a long side chain are included in products of catalytic cracking of polycyclic aromatic hydrocarbons which are one class of main components of heavy oil.[2-4] Except ethylbenzene, monoaromatic hydrocarbons with long alkyl chains are not so useful chemicals and are mainly used as fuel. Such monoaromatic hydrocarbons are also present in heavy naphtha (5-10%), and the amount is increased by reforming (about twice).[5,6] Although the percentages are not so high, the absolute amount is quite large because heavy naphtha is utilized in very large scale. On the other hand, aromatics with methyl groups, especially *p*-xylene, are highly useful chemicals. Therefore, conversion of the alkyl groups of monoaromatic hydrocarbons to methyl groups is a valuable process; however, such process has been hardly reported. Conventional methods for C-C dissociations include thermal cracking, catalytic cracking and hydrocracking (hydrogenolysis).[7,8] The main products of both thermal cracking and catalytic cracking of aromatic hydrocarbons with long side chains are not methylbenzenes: formation of styrenes[9] and dissociation of C_{aryl}-C_{alkyl} bond[10,11] proceeds instead, respectively. There are several hydrogenolysis systems of aromatic hydrocarbons. Reactions of tetralin over metal-acid bifunctional catalysts such as noble metal/zeolite,[12,13] noble metal/SiO_2-Al_2O_3,[14] noble metal/SiO_2-ZrO_2,[15] and Ni/zeolite[16] are typical examples. Ni-Mo catalysts with acidic property, which are analogues of hydrodesulfurization catalysts, are also tested as bifunctional catalysts for hydrogenolysis.17,18 These bifunctional catalysts cleave the C-C bond mainly via

Friedel-Crafts-type reaction over the acid sites, and C_{aryl}-C_{alkyl} bond is preferably dissociated (butylbenzene from tetralin). In addition, bifunctional catalysts have hydrogenation activity and the benzene ring tends to be hydrogenated, especially at lower reaction temperature. Recently, the use of H-beta as acid component such as Ni/H-beta has been reported to produce BTX fractions in significant yield at high reaction temperature (~673 K),[19,20] and the reported yields of toluene + xylenes from tetralin are 20~30%.[21,22] On the other hand, monofunctional metal catalysts were also tested for C-C bond cleavage by hydrogenolysis.[23] Ir, Rh and Ru are typical active metals, and Ru is known to have higher activity.[24] Recently, we have developed Ru/CeO_2 catalyst with very small Ru particles (< 1.5 nm) prepared by treatment with inert gas at 573 K after impregnation.[25,26] This C-C dissociation catalyst shows good regioselectivity toward inner C-C bonds instead of terminal C-C bonds of alkanes.[25-27] We also developed Ru-VO_x/SiO_2 catalyst with small Ru ensembles which give similar good regioselectivity, although the modification of V decreases the activity of Ru.[28] Because of the high hydrogenation activity, the monofunctional catalysts have been mainly applied to saturated substrates such as naphthenes, higher *n*-alkanes and hydrogenated terpenoids, and the C-C dissociations of aromatic substrates are hardly tested. In this paper, we tested various noble metal catalysts including Ru/CeO_2 for hydrogenolysis of C-C bods in alkyl chain of monoaromatics. We found that Ru/CeO_2 catalyst with appropriate Ru loading can effectively convert ethylbenzene to toluene (eq. (1)) with suppression of ring hydrogenation (eq. (2)) and C_{aryl}-C_{alkyl} dissociation (eq. (3)) under appropriate reaction conditions. Production of *p*-xylene from 4-ethyltoluene (eq. (4)) is also possible with this catalyst.

$C_6H_5C_2H_5(g) + H_2 \rightarrow C_6H_5CH_3(g) + CH_4 \quad \Delta H^\circ_{298} = -55 \text{ kJ mol}^{-1}, \Delta G^\circ_{298} = -53 \text{ kJ mol}^{-1}$ (1)

$C_6H_5C_2H_5(g) + 3H_2 \rightarrow C_6H_{11}C_2H_5(g) \quad \Delta H^\circ_{298} = -203 \text{ kJ mol}^{-1}, \Delta G^\circ_{298} = -92 \text{ kJ mol}^{-1}$ (2)

$C_6H_5C_2H_5(g) + H_2 \rightarrow C_6H_6(g) + C_2H_6 \quad \Delta H^\circ_{298} = -31 \text{ kJ mol}^{-1}, \Delta G^\circ_{298} = -17 \text{ kJ mol}^{-1}$ (3)

$p\text{-}CH_3C_6H_4C_2H_5 + H_2 \rightarrow p\text{-}CH_3C_6H_4CH_3 + CH_4$ (4)

2. Experimental section

2.1. Catalyst preparation

Ru/support catalysts (Ru: typically 4 wt%) were prepared by impregnation method with various supports and $Ru(NO)(NO_3)_{3-x}(OH)_x$ in diluted nitric acid (Sigma Aldrich). Supports used in experiment were as follows: SiO_2 (Fuji Silysia Chemical Ltd., G-6, calcined at 973 K for 1 h), CeO_2 (Daiichi Kigenso Kagaku Kogyo Co., Ltd., HS, calcined for 3 h (typically 1073 K)), Al_2O_3 (Nippon Aerosil Co., Ltd., AEROXIDE Alu C, calcined at 973 K for 1 h), MgO (Ube Industries Ltd., 500A, calcined at 973 K for 1 h), TiO_2 (Nippon Aerosil Co., Ltd., AEROXIDE P25, calcined at 973 K for 1 h), and ZrO_2 (Daiichi Kigenso Kagaku Kogyo Co., Ltd., RC-100P, calcined at 973 K for 1 h). M/CeO_2 (M = Rh, Ir, Pt, Pd; M 4 wt%) were also prepared by impregnation method with various precursors. Metal precursors used in experiment were as follows: $Rh(NO_3)_3$ (Wako Pure Chemicals Industries, Ltd.), $Ir(NO_3)_3$ (Furuya Metal Co., Ltd.), $Pt(NO_2)_2(NH_3)_2$ (Tanaka Kikinzoku Kogyo), $Pd(NO_3)_2$ (N.E. CHEMCAT Corp.). After evaporating the solvent, all the prepared catalysts were dried at 383 K for 12 h, and pretreated for 1 h in N_2 flow at 573 K. The catalysts are denoted as

M(*m*)/support^n, where *m* and *n* represents the loading amount in wt% for M and the calcination temperature in K for support, respectively.

2.2. Activity tests

Hydrogenolysis of ethylbenzene (Tokyo Chemical Industry Co., Ltd., > 99%), 4-ethyltoluene (Tokyo Chemical Industry Co., Ltd., > 95%), propylbenzene (Tokyo Chemical Industry Co., Ltd., > 99%), cumene (Tokyo Chemical Industry Co., Ltd., > 99%), *p*-xylene (Wako Pure Chemicals Industries, Ltd., > 98%) and toluene (Wako Pure Chemicals Industries, Ltd., > 99.5%) was performed in a fixed-bed quartz tube reactor under atmospheric pressure. Before the activity test, the catalyst (100 mg; 60-80 mesh) was reduced at 533 K for 0.5 h in H_2 flow (50 ml/min). After the pretreatment, the feed gas was changed to hydrocarbon/N_2/H_2 (typically in a 1:26:78 molar ratio, total gas feed rate 128 mmol h^{-1} (W/F=0.8 g$_{-\mathrm{cat}}$ h^{-1} mol$_{-\mathrm{total}}{}^{-1}$)). The feed was maintained for 2 h to reach a steady state. The product gas was collected in a hot syringe heated at 353 K and analyzed with GC (Shimadzu GC-2014) equipped with flame ionization detector (FID). An Rtx®-1 PONA column (Restek Corp.) was used for separation. 0.1 ml of gas sample was injected into GC. The conversion and selectivity were calculated on carbon-basis with eqs. (5) and (6) as shown below. The carbon balance (eq. (7)) was always in the range of the experimental error (±10%), except in the cases of low conversion of substrate where the carbon balance was sometimes fluctuated (120% in the worst case) probably because of the condensation of substrate. In the cases of very high conversion level (>90%), the conversion was calculated by the decrease of substrate amount instead of eq. (5).

$$\text{Conversion (\%)}=\left(\frac{\sum \text{Amount of products [mol-C]}}{\text{Amount of substrate input [mol-C]}}\right)\times 100 \quad (5)$$

$$\text{Selectivity (\%)}=\left(\frac{\text{Amount of each product [mol-C]}}{\sum \text{Amount of products [mol-C]}}\right)\times 100 \quad (6)$$

$$\text{Carbon balance (\%)}=\left(\frac{\text{Amount of unreacted substrate [mol-C]}+\sum \text{Amount of products [mol-C]}}{\text{Amount of substrate input [mol-C]}}\right)\times 100 \quad (7)$$

2.3. Characterization

BET surface area was measured with Micromeritics Gemini VII 2390 instrument. H_2 temperature programmed reduction (H_2-TPR) was carried out in a fixed-bed reactor equipped with a thermal conductivity detector (TCD) and frozen acetone trap using 5% H_2 diluted with Ar (30 ml/min). The amount of sample was 0.05 g or 0.1 g, and the temperature was increased from 223 K (cooled with frozen acetone) to 973 K at a heating rate of 10 K/min. Thermogravimetry-differential thermal analysis (TG-DTA) was carried out with a Rigaku Thermo Plus EVO-II under air atmosphere. X-ray diffraction (XRD) patterns were recorded by a diffractometer (Rigaku MiniFlex600). Cu K_α (λ = 0.154 nm, 45 kV, 40 mA) radiation was used as an X-ray source. The amount of H_2 chemisorption was measured in a high-vacuum system using a volumetric method in a vacuum line. Before adsorption measurements, the catalysts were reduced with H_2 at 533 K for 2 h. The adsorption was conducted at room temperature and the final H_2 pressure was about 4 kPa. The measurement of H_2 adsorption was repeated after evacuation at room temperature in order to determine the physisorption amount. The chemisorption amount was determined by the difference of these two adsorption amounts. Transmission electron microscope (TEM) images were obtained on a

JEOL JEM-2100F (for Ru/CeO_2 samples) or Hitachi HD-2700 (for Ru/(other support) samples) instrument. The catalysts after the reduction with H_2 at 533 K or after reaction were used as samples for the TEM observation. The samples were dispersed in ethanol under supersonic waves and were dropped on grids. X-ray photoelectron spectra (XPS) were measured with Shimadzu AXIS-ULTRA DLD spectrometer under high vacuum at room temperature. The catalyst sample was mixed with SiO_2 (1:1 in weight), and pressed into a disk. The disk was reduced with H_2 at 533 K for 0.5 h, and transferred to the measurement chamber in inert atmosphere. The binding energy was corrected by Si 2s peak at 154.4 eV because of the overlap between C 1s and Ru $3d_{3/2}$ signals.

3. Results and discussion

3.1. Hydrogenolysis of ethylbenzene over noble metal catalysts

Ethylbenzene was selected as a model substrate in this study (eq. (1)). The target product is toluene, and the maximum carbon-based selectivity of toluene is 88% (=7/8). Methane is always co-produced with toluene (methane:toluene carbon ratio = 1:7), while some side reactions also produce methane. Ethylcyclohexane (ECH) and methylcyclohexane (MCH) are main by-products via hydrogenation of benzene ring. Other by-products are benzene, cyclohexane, and smaller hydrocarbons that are produced by overhydrogenolysis. Figure 1 shows the results of hydrogenolysis of ethylbenzene over 4 wt% noble metal catalysts supported on CeO_2 pre-calcined at 1073 K (M(4)/CeO_2^{1073}). Ru catalyst showed the highest activity among the tested noble metal catalysts: The conversion level over Ru(4)/CeO_2^{1073} was comparable or higher than those over other M(4)/CeO_2^{1073} catalysts at one fourth of contact time. The selectivity to toluene over Ru(4)/CeO_2^{1073} was higher than those over other noble metal catalysts, and the high selectivity was almost maintained at higher conversion level. The carbon ratio of produced methane:toluene (1:5.9 at 40% conversion) was only slightly smaller the stoichiometrical one (1:7), indicating that amount of methane produced by side-reactions was small. Rh and Ir catalysts showed some activity in toluene formation; however, ethylcyclohexane was also formed in similar selectivity to toluene. In the cases of Pd and Pt catalysts, the main product was ethylcyclohexane. Therefore, Ru is the most suitable active metal species for hydrogenolysis of ethylbenzene to toluene without hydrogenation of the benzene ring.

Next, we investigated the effect of support for Ru catalysts in hydrogenolysis of ethylbenzene. Figure 2 shows the reaction results over various Ru(4)/support catalysts. All the tested Ru catalysts showed good selectivity to toluene. The activity much depended on the used support. CeO_2 supports gave much higher activity than other supports. This is in contrast to the hydrogenolysis of alkanes where Ru(4)/CeO_2^{873} catalyst shows significantly lower activity than Ru(4)/SiO_2^{973} catalyst.[25-27] As described later, the higher activity of Ru/CeO_2 than other Ru catalysts shown in Figure 2 can be mostly (although not totally) explained by the difference of dispersion. The dependence of the performance of Ru(4)/CeO_2 catalysts on the calcination temperature of support was also investigated, and Ru(4)/CeO_2^{1073} showed the highest activity (The performances of Ru(4)/CeO_2^{673} and Ru(4)/CeO_2^{1273} are shown in Figure S1, supporting information). According to our previous reports on the CeO_2 catalysts, CeO_2 calcined at 873 K or higher temperature has sufficiently high crystallinity, and higher calcination temperature than 873 K simply decreases both the surface area and catalytic activity in acid/base reactions.[29] In order to further investigate the effect of calcination temperature of CeO_2 support, the Ru loading amount was also changed for both CeO_2^{873} (pre-calcined at 873 K; BET surface area 83 m^2 g^{-1}) and CeO_2^{1073} (41 m^2 g^{-1}) supports. The results of the reaction tests are shown in Figure 3. The activity (conversion) fairly corresponded to the Ru loading amount. In view of selectivity, considering that selectivity to toluene was gradually decreased at higher conversion level, catalysts with low Ru loading amount showed much lower selectivity to toluene, and ethylcyclohexane became the main product instead. The selectivity change suddenly occurred at some level of Ru loading amount: For CeO_2^{1073} support, the selectivity change occurred between Ru loading amount of 0.5 and 1 wt%, while for CeO_2^{873} support it occurred between 1 and 4 wt%. Considering that the surface area of CeO_2^{873} is about twice of that of CeO_2^{1073}, the selectivity of Ru/CeO_2 is suggested to be determined by the Ru concentration on the CeO_2 surface ([Ru loading amount]/[surface area of CeO_2 support]). High Ru surface concentration on CeO_2 above ~1 atom/nm^2 (corresponding to 0.75 wt% Ru on support with 40 m^2 g^{-1} surface area) gives good selectivity to toluene. After all, we selected Ru(4)/CeO_2^{1073} as the optimized catalyst for this reaction.

3.2. Optimization of reaction conditions

Figure 4 shows the effect of reaction temperature on hydrogenolysis of ethylbenzene over Ru(4)/CeO_2^{1073}. Lower reaction temperature (513 K) gave higher selectivity to ethylcyclohexane which is the hydrogenation product of the benzene ring. In view of both activity and selectivity, 533 K is better reaction temperature than 513 K. Here, it should be discussed whether the equilibrium of ring hydrogenation/dehydrogenation limited the formation of ethylcyclohexane or not. In Figure 1, Pt/CeO_2 catalyst showed almost 100% selectivity to ethylcyclohexane at 40% conversion at 533 K, which means that the equilibrium limitation of the ethylcyclohexane formation is not lower than this yield. On the other hand, $Ru(4)/CeO_2^{1073}$ catalyst showed <10% selectivity to ethylcyclohexane at similar conversion level. Therefore, the formation amount of ethylcyclohexane over $Ru(4)/CeO_2^{1073}$ was much lower than the equilibrium level, at least in the case of 533 K. The high selectivity to toluene and low selectivity to ethylcyclohexane were kinetically controlled.

At 553 K, the activity was increased from 533 K; however, the difference was not so large. The selectivity to toluene was similar to that at 533 K. The smaller increase of activity between 533 and 553 K than between 513 and 533 K may be due to the decrease of substrate coverage on the active site at higher temperature. The selectivity to ethylcyclohexane was decreased and those to smaller hydrocarbons including methane were increased instead. Considering the decrease of selectivity to ethylcyclohexane from 513 K to 533 K, the very low selectivity to ethylcyclohexane at 553 K was probably due to the suppression of hydrogenation of benzene ring rather than rapid overhydrogenolysis of ethylcyclohexane. However, overhydrogenolysis of toluene to smaller hydrocarbons more proceeded at high conversion levels at 553 K, and the toluene yield at 553 K was rather lower than that 533 K. We selected 533 K as the standard reaction temperature.

In our previous report,[26] hydrogenolysis of alkanes over $Ru(5)/CeO_2^{873}$ was carried out at much lower reaction temperature (433 K) under similar flow conditions (W/F ~0.1 g_{cat} h^{-1} mol^{-1}, alkane:N_2:H_2 ~ 1:60:60, ambient pressure). The conversion of *n*-hexane at W/F = 0.08

g_{cat} h^{-1} mol^{-1} was about 20%, and about 40 mol% of the total products was methane.[26] These data indicate that the reactivity to ethylbenzene is much lower than *n*-alkanes. Strong adsorption of benzene ring on the catalyst surface may lower the reactivity to hydrogenolysis over Ru.

Figure 5 shows the effect of H_2:N_2 ratio (H_2 partial pressure) on hydrogenolysis of ethylbenzene. Higher H_2 concentration (higher H_2/N_2 ratio) gave higher activity. Although the selectivity to ethylcyclohexane was slightly increased with increase of H_2 concentration, we selected H_2/N_2 ratio = 3 ($P(H_2) = 0.075$ MPa) as the standard reaction conditions because of the high reaction rate. Too high H_2 pressure may lead to high selectivity to ring-hydrogenated products. In fact, hydrogenation of aromatic ring over Ru/CeO_2 catalysts under high-pressure H_2 (a few MPa) in batch reactor has been reported.[30,31] At 533 K under $H_2/N_2 = 3$, 65% yield of toluene (theoretical maximum = 88%) was obtained at $W/F = 0.4$ g_{cat} h^{-1} mol^{-1}. This value is much higher than the reported yield values (<~30%) of toluene + xylene by hydrocracking of aromatics.[21,22] Longer contact time (W/F) increased the selectivity to smaller hydrocarbons including methane and decreased the selectivity to toluene.

The effect of substrate (ethylbenzene) partial pressure was also investigated, and the detailed data are shown in Table S1. The selectivity pattern was not changed by the substrate partial pressure for both Ru(4)/CeO_2^{1073} and Ru(0.5)/CeO_2^{1073}. The substrate partial pressure has weak positive effect on the activity; the reaction order with respect to ethylbenzene partial pressure was about 0.3 for both catalysts, indicating that the active sites on the both catalysts fairly adsorbed the ethylbenzene molecule. The low reaction order was consistent with the data that almost total conversion was obtained in Figures 4 and 5.

3.3. Hydrogenolysis of other substrates

The hydrogenolysis system of Ru(4)/CeO_2^{1073} catalyst was applied to various aromatic hydrocarbons (Table 1). Because hydrogenolysis of *p*-dialkylbenzenes can give *p*-xylene which is a very important raw material of PET, we carried out hydrogenolysis of *p*-ethyltoluene (Table 1, entries 5-8). The reactivity of *p*-ethyltoluene was slightly lower than that of ethylbenzene. The highest *p*-xylene selectivity was 53% (theoretical maximum = 8/9 = 89%), which was obtained around $W/F = 0.4\sim0.8\ g_{cat}\ h^{-1}\ mol^{-1}$.

In the case of propylbenzene (Table 1, entries 9-11), both toluene and ethylbenzene were formed, and toluene was more formed (toluene/ethylbenzene molar ratio ~ 3) (Scheme 1A). Comparable amount of ethane to toluene was actually detected (ethane/toluene molar ratio ~ 0.7), which indicated that most toluene was produced by direct dissociation of PhC-C bond rather than stepwise hydrogenolysis via ethylbenzene. The ratios were gradually changed by the overhydrogenolysis of ethylbenzene. The reactivity of propylbenzene was much lower than those of ethylbenzene and *p*-ethyltoluene.

Hydrogenolysis of cumene (isopropylbenzene) gave ethylbenzene as the main product at short contact time (Table 1, entry 12). As the contact time was increased, the selectivity to ethylbenzene was decreased and that to toluene was increased, suggesting that toluene was mainly produced by successive hydrogenolysis via ethylbenzene (Table 1, entries 12-14) (Scheme 1B). The reactivity of cumene was also lower than those of ethylbenzene and 4-ethyltoluene.

The reactions of target products, toluene and *p*-xylene, were also investigated (Table 1, entries 15 and 16). The reactivities were surely lower than alkylbenzenes with ≥C2 alkyl chains. In particular, hydrogenolysis of toluene to benzene was very slow, and rather hydrogenation to methylcyclohexane more proceeded. The results agreed with that benzene was hardly formed from ethylbenzene, propylbenzene and cumene. On the other hand, the main product from *p*-xylene was toluene, and the selectivity to ring-hydrogenated products was low. The adsorption of the substrate with the benzene ring might be blocked to some extent by the two methyl groups.

The reactivity and selectivity trends are related to the reaction mechanism. According to the literature[32] and our previous studies,[26] the C-C hydrogenolysis of alkanes over metal surface starts with dissociation of C-H bond and formation of C-metal bond. In alkylbenzenes, the weakest C-H bond is that at the benzyl position, and thus (Ph-)C-metal bond is preferably formed. Next, the dissociation of C-C bond produces two alkyl or alkylidene surface species in hydrogenolysis of alkanes. In the case of ethylbenzene (Scheme 2A), $PhCH(CH_3)$- surface species is formed first. There can be two C-C dissociation reactions: formation of Ph- + C_2H_5- surface species and that of PhCH- + CH_3- surface species. The former pair of surface species is less stable than the latter pair because C-H bond in benzene ring is much stronger than that at the benzyl position. Therefore toluene and methane are the main products from ethylbenzene. In the case of propylbenzene, the main reaction is the formation of toluene and ethane in similar mechanism. However, the steric hindrance around the benzyl position can weaken the formation of the surface intermediate species, leading to the lower reactivity than ethylbenzene. In the case of *p*-ethyltoluene (Scheme 2B), *p*-$CH_3C_6H_4CH(CH_3)$- surface species is the precursor of *p*-xylene. However, *p*-$C_2H_5C_6H_4CH_2$- surface species can be also formed, which is not reactive in further hydrogenolysis. The competitive formation of these surface species can decrease the reactivity of *p*-ethyltoluene in comparison with ethylbenzene.

3.4. Catalyst stability

We conducted the stability test of Ru(4)/CeO_2^{1073} for hydrogenolysis of ethylbenzene (Figure 6). The conversion and selectivity pattern were not changed. Thermogravimetric (TG) analysis of the used catalyst showed that the amount of deposited organic substance (coke) was negligible (Figure S2). The TEM image of the used catalyst was also essentially unchanged from the fresh reduced catalyst (Figure S3). These results indicate that the Ru(4)/CeO_2^{1073} catalyst is stable during hours of use. The good stability of Ru/CeO_2 catalyst for hydrocarbon hydrogenolysis has been also reported in alkane hydrogenolysis in both batch and fixed-bed reactions.[25-27]

3.5. Catalyst characterization

The Ru catalysts on various supports were characterized by N_2 adsorption (BET surface area), XRD, TEM and H_2 chemisorption. The results are summarized in Table 2, and the raw data are shown in Figures S4 (XRD) and S5 (TEM). Although measurement of Ru particles was not possible for all catalysts with XRD and TEM because of the detection limit or the overlap of signals with support, the size of Ru particles determined by XRD and TEM fairly agreed with the dispersion determined by H_2 chemisorption (H/Ru). From the comparison between the dispersion and activity, higher activity of Ru(4)/CeO_2 catalysts than other Ru(4) catalysts can be mostly explained by the higher dispersion. However, the activity of

Ru/support catalysts cannot be explained only by dispersion. Catalysts with acidic support such as Al_2O_3 have relatively lower activity.

As described in section 3.1 and Figure 3, the selectivity of Ru/CeO_2 catalyst much depends on the concentration of Ru on the surface of CeO_2 support, and higher concentration gives higher selectivity to toluene from ethylbenzene. From Table 2, there is little correlation between the selectivity and dispersion of the six Ru/CeO_2 catalysts. Therefore we further characterize the Ru/CeO_2 catalysts with different Ru loadings.

The H_2-TPR profiles of Ru/CeO_2^{1073} catalysts are shown in Figure 7. All the catalysts showed reduction signals below 473 K, and thus the reduction completed below the reaction temperature (≥513 K). The H_2 consumption amount was 0.40, 0.56 and 1.4 mmol g^{-1} for $Ru(0.5)/CeO_2^{1073}$, $Ru(1)/CeO_2^{1073}$ and $Ru(4)/CeO_2^{1073}$, respectively, and was higher than the amount required for the reduction of oxidized Ru such as RuO_2 to Ru metal. The surface of CeO_2 was also reduced. The reduction temperature was similar for all the Ru/CeO_2^{1073} catalysts.

The TEM images of reduced Ru/CeO_2^{1073} catalysts are shown in Figure 8. In Figure 8(a) and (b) which represents $Ru(4)/CeO_2^{1073}$ and $Ru(1)/CeO_2^{1073}$, respectively, Ru particles are clearly observed. On the other hand, in $Ru(0.5)/CeO_2^{1073}$ catalyst, which has relatively high activity in benzene ring hydrogenation and low selectivity to toluene, Ru particles were not observed. The Ru species in $Ru(0.5)/CeO_2^{1073}$ is too small in particle size or amorphous. We also carried out XAFS measurement of reduced Ru/CeO_2^{1073} catalysts to determine the coordination environment of the Ru particles. However, in spite of repeated trials for the measurement of reduced catalysts without exposure to air, the obtained Ru *K*-edge spectrum of Ru(0.5)/CeO_2^{1073} were always the pattern of oxidized Ru species (Figure S6). Considering the TPR results, it is unlikely that the Ru species are not reduced by the treatment with H_2 at 533 K. The Ru species in Ru(0.5)/CeO_2^{1073} catalyst is probably very easily oxidized by trace O_2 (cf. the detection limit of O_2 meter in the glove bag was 0.1%; carrying the sample reduced in our lab to the synchrotron apparatus took a few days). The absence of Ru particles in TEM image of Ru(0.5)/CeO_2^{1073} catalyst (Figure 8(c)) agrees with the idea that the Ru species is very easily oxidized with air. On the other hand, the XAFS spectra of Ru(4)/CeO_2^{1073} and Ru(1)/CeO_2^{1073} were the patterns of metallic Ru, and the Ru-Ru coordination numbers (CNs) in EXAFS curve fitting analysis were 7.8 and 4.2, respectively (Table S2). The much lower CNs than that of bulk Ru (CN = 12) agreed with the formation of small Ru particles (< 2 nm) as observed in TEM.

We also carried out XPS measurement of the reduced catalysts (Figure S7). The samples after reduction were quickly transferred to vacuum chamber in inert atmosphere. All the catalysts including Ru(0.5)/CeO_2^{1073} and Ru(0.5)/CeO_2^{873} showed stronger signal of metallic Ru^0 than that of $Ru^{IV}O_2$ in Ru $3d_{5/2}$ region, confirming that Ru was surely reduced to the metallic state by heating under H_2. The peak position of Ru^0 signal seems to be shifted to lower binding energy (~0.3 eV) by decreasing the Ru loading amount, suggesting that the electronic state of Ru particles was negatively charged in low Ru loading due to reduced CeO_2 surface. However, the determination of the electronic state of metallic Ru species by these spectra is not decisive because there was still some signal of oxidized Ru species; surface oxidation of Ru particles probably proceeded during the sample transfer process, and the electronic state of Ru metal particles can be changed by this oxidation. We do not include the detailed curve-deconvolution results of these XPS data, because we do not think that the ratio of Ru^{n+}/Ru^0 in the data represents the exact state of reduced catalysts.

In the three Ru/CeO_2^{1073} catalysts, only $Ru(0.5)/CeO_2^{1073}$ showed low selectivity to toluene. Similarly, for Ru/CeO_2^{873} catalysts, $Ru(1)/CeO_2^{873}$ and $Ru(0.5)/CeO_2^{873}$ which had low selectivity to toluene showed XAFS spectra of oxidized Ru species, while Ru metal was detected in XAFS spectra of $Ru(4)/CeO_2^{873}$ which had good selectivity to toluene. The Ru species that are easily oxidized by O_2 seem to have activity in hydrogenation of benzene ring.

Here, the TEM images are closely investigated again. The Ru particles in $Ru(4)/CeO_2^{1073}$ are block-shaped (Figure 8(a)). On the other hand, the Ru particles in $Ru(1)/CeO_2^{1073}$ are low hill-shaped. The relatively large number of particles in $Ru(1)/CeO_2^{1073}$ considering the much lower Ru loading amount than $Ru(4)/CeO_2^{1073}$ indicates the small volume of each Ru particle, agreeing with the low shape. Lower height of supported particles means that they are more sensitive to the electronic effect by the support. Lowering the Ru loading amount decreases the height of supported particles rather than decreases the particle size with similar shape. Further lowering the Ru loading amount can give thin flat particles. The electronic state of such particles is highly affected by the CeO_2 support, and the particles are very easily oxidized. The flat particles have activity in benzene ring hydrogenation. The schematic representation of catalyst structure and catalytic performance described above are summarized in Figure 9. The hydrogenation activity of flat Ru species on low-loading-amount Ru/CeO_2 catalysts can be due to electronic effect by the CeO_2 support or geometric effect of flat Ru surface that can adsorb flat aromatic ring. Considering that very large Ru particles which also have flat Ru surface have low hydrogenation selectivity, the electronic effect by the CeO_2

surface is more plausible. Although the hydrogenation is not the target reaction in this work, the investigation of the electronic effect can be an interesting topic in future works.

4. Conclusions

Ru(4)/CeO_2^{1073} catalyst (4 wt% Ru loading on CeO_2 support pre-calcined at 1073 K) shows good activity and selectivity in hydrogenolysis of ethylbenzene to toluene with suppressing hydrogenation of the benzene ring. Catalysts supporting another noble metal showed significant selectivity to ring-hydrogenation products. The highest yield of toluene was 65 %-C (theoretical maximum yield: 88 %-C) at 533 K and H_2 partial pressure of 0.075 MPa over Ru(4)/CeO_2^{1073} catalyst. This yield value is much higher than those of methylbenzenes yield from large alkylbenzenes in literature hydrogenolysis systems such as Ni/H-beta. The selections of reaction temperature and H_2 pressure are very important: too low temperature and too high H_2 pressure increases selectivity to ring-hydrogenated products; too high temperature promotes overhydrogenolysis to smaller hydrocarbons; and too low H_2 pressure decreases the activity. The catalyst has excellent stability during hours of reaction, and no coke deposition was observed. Other aromatic hydrocarbons with ≥C2 chains were also converted to methylated aromatic hydrocarbons. The reactivity of aromatic hydrocarbons with C3 chain is lower than that of ethylbenzene probably because of the steric hindrance. The good activity of Ru(4)/CeO_2^{1073} catalyst is due to the high dispersion of Ru particles. However, the interaction of Ru particles and CeO_2 is not wholly advantageous to the catalysis: too low loading amount of Ru on CeO_2 support gives hydrogenation activity of benzene ring to the catalyst by formation of Ru particles highly interacted with CeO_2 support.

Acknowledgements

We thank the Technical Division in School of Engineering, Tohoku University for TEM and XPS measurements.

References

[1] M. S. Rana, V. Sámano, J. Ancheyta, J. A. I. Diaz, *Fuel* **2007**, *86*, 1216-1231.

[2] Y. Miki, Y. Sugimoto, *Fuel Proc. Technol.* **1995**, *43*, 137-146.

[3] I. Shimada, K. Takizawa, H. Fukunaga, N. Takahashi, T. Takatsuka, *Fuel* **2015**, *161*, 207-214.

[4] R. Pujro, M. Falco, U. Sedra, *Energy Fuels* **2015**, *29*, 1543-1549.

[5] J. Ancheyta-Juárez,; E. Villafuerte-Marcías, L. Díaz-García, E. González-Arredondo, *Energy Fuels* **2001**, *15*, 887-893.

[6] A. A. Al-Shammari, S. A. Ali, N. Al-Yassir, A. M. Aitani, K. E. Ogunronbi, K. A. Al-Majnouni, S. S. Al-Khattaf, *Fuel Proc. Technol.* **2014**, *122*, 12-22.

[7] A. Corma, B. W. Wojciechowski, *Catal. Rev.* **1985**, *27*, 29-150.

[8] J. Weitkamp, *ChemCatChem* **2012**, *4*, 292-306.

[9] Q. Chen, G. F. Froment, *J. Anal. Appl. Pyrolysis* **1991**, *21*, 51-77.

[10] H. B. Mostad, T. Riis, O. H. Ellestad, *Appl. Catal.* **1990**, *63*, 345-364.

[11] A. T. Townsend, J. Abbot, *Appl. Catal. A* **1992**, *90*, 97-115.

[12] M. J. Girgis, Y. P. Tsao, *Ind. Eng. Chem. Res.* **1996**, *35*, 386-396.

[13] S. J. Ardakani, K. J. Smith, *Appl. Catal. A* **2011**, *403*, 36-47.

[14] a) S. Nassreddine, L. Massin, M. Aouine, C. Geantet, L. Piccolo, *J. Catal.* **2011**, *278*, 253-265; b) L. Piccolo, S. Nassreddine, M. Aouine, C. Ulhaq, C. Geantet, *J. Catal.* **2012**, *292*, 173-180.

[15] E. Rodríguez-Castellón, J. Mérida-Robles, L. Díaz, P. Maireles-Torres, D. J. Jones, J. Rozière, A. Jiménez-López, *Appl. Catal. A* **2004**, *260*, 9-18.

[16] Y. Wang, B. Shen, L. Wang, B. Feng, J. Li, Q. Guo, *Fuel Proc. Technol.* **2013**, *106*, 141-148.

[17] R. Hernández-Huesca, J. Mérida-Robles, P. Maireles-Torres, E. Rodríguez-Castellón, A. Jiménez-López, *J. Catal*. **2001**, *203*, 122-132.

[18] S. G. A. Ferraz, B. M. Santos, F. M. Z. Zotin, L. R. R. Araujo, J. L. Zotin, *Ind. Eng. Chem. Res.* **2015**, *54*, 2646-2656.

[19] G. C. Laredo, P. Pérez-Romo, J. Escobar, J. L. Garcia-Gutierrez,; P. M. Vega-Merino, *Ind. Eng. Chem. Res.* **2017**, *56*, 10939-10948.

[20] Y.-S. Kim, K.-S. Cho, Y.-K. Lee, *J. Catal.* **2017**, *351*, 67-78.

[21] a) Y. Choi, J. Lee, J. Shin, S. Lee, D. Kim, J. K. Lee, *Appl. Catal. A* **2015**, *492*, 140-150; b) J. Lee, Y. Choi, J. Shin, J. K. Lee, *Catal. Today* **2016**, *265*, 144-153; c) J. Shin, Y. Oh, Y. Choi, J. Lee, J. K. Lee, *Appl. Catal. A* **2017**, *547*, 12-21.

[22] D. P. Upare, S. Park, M. S. Kim, Y.-P. Jeon, J. Kim, D. Lee, J. Lee, H. Chang, S. Choi, W. Choi, Y.-K. Park, C. W. Lee, *J. Ind. Eng. Chem.* **2017**, *46*, 356-363.

[23] G. C. Bond, *Metal-Catalyzed Reactions of Hydrocarbons*, Springer, New York, **2005**.

[24] G. B. McVicker, M. Daage, M. S. Touvelle, C. W. Hudson, D. P. Klein, W. C. Baird, B. R. Cook, J. G. Chen, S. Hantzer, D. E. W. Vaughan, E. S. Ellis, O. C. Feeley, *J. Catal.* **2002**, *210*, 137-148.

[25] S. Oya, D. Kanno, H. Watanabe, M. Tamura, Y. Nakagawa, K. Tomishige, *ChemSusChem* **2015**, *8*, 2472-2475.

[26] Y. Nakagawa, S. Oya, D. Kanno, Y. Nakaji, M. Tamura, K. Tomishige, *ChemSusChem* **2017**, *10*, 189-198.

[27] Y. Nakaji, S. Oya, H. Watanabe, M. M. Watanabe, Y. Nakagawa, M. Tamura, K. Tomishige, *ChemCatChem* **2017**, *9*, 2701-2708.

[28] Y. Nakaji, Y. Nakagawa, M. Tamura, K. Tomishige, *Fuel Proc. Technol.* **2018**, *176*, 249-257.

[29] (a) Y. Yoshida, Y. Arai, S. Kado, K. Kunimori, K. Tomishige, *Catal. Today* **2006**, *115*, 95-101; (b) M. Honda, A. Suzuki, B. Noorjahan, K. Fujimoto, K. Suzuki, K. Tomishige, *Chem. Commun.* **2009**, 4596-4598; (c) M. Honda, S. Kuno, S. Sonehara, K. Fujimoto, K. Suzuki, Y. Nakagawa, K. Tomishige, *ChemCatChem* **2011**, *3*, 365-370; (d) M. Honda, M. Tamura, Y. Nakagawa, S. Sonehara, K. Suzuki, K. Fujimoto, K. Tomishige, *ChemSusChem* **2013**, *6*, 1341-1344.

[30] R. S. Suppino, R. Landers, A. J. G. Cobo, *Appl. Catal. A* **2013**, *452*, 9-16.

[31] T. Mizugaki, K. Togo, Z. Maeno, T. Mitsudome, K. Jitsukawa, K. Kaneda, *Sci. Rep.* **2017**, *7*, 14007.

[32] (a) D. W. Flaherty, E. Iglesia, *J. Am. Chem. Soc.* **2013**, *135*, 18586-18599; (b) D. W. Flaherty, D. D. Hibbitts, E. Iglesia, *J. Am. Chem. Soc.* **2014**, *136*, 9664-9676.

Table 1. Hydrogenolysis of various aromatic hydrocarbons over Ru(4)/CeO_2^{1073} [a]

Entry	Substrate	*W*/*F* [g_{cat} h mol^{-1}]	Conv. [%]	Selectivity [%-C]						
				p-Xy	EB	T	B	Hy	Methane	Others
1	Ethylbenzene	0.1	40	-	-	77	2	7	13	1
2	Ethylbenzene	0.2	73	-	-	77	2	8	10	3
3	Ethylbenzene	0.4	95	-	-	69	3	8	15	5
4	Ethylbenzene	0.8	99	-	-	53	4	12	20	11
5	*p*-Ethyltoluene	0.1	22	73	3	7	<1	2	14	<1
6	*p*-Ethyltoluene	0.2	53	72	3	9	<1	2	13	2
7	*p*-Ethyltoluene	0.4	76	69	1	12	1	2	14	2
8	*p*-Ethyltoluene	0.8	99	54	<1	19	1	2	18	6
9	Propylbenzene	0.2	13	-	17	45	1	15	12	10(9[b])
10	Propylbenzene	0.4	27	-	15	44	1	15	10	16(8[b])
11	Propylbenzene	0.8	41	-	12	42	2	12	14	18(9[b])
12	Cumene	0.2	27	-	49	23	1	8	16	4
13	Cumene	0.4	42	-	33	35	1	4	20	7
14	Cumene	0.8	81	-	9	48	3	4	27	9
15	Toluene	0.4	20	-	-	-	15	37	20	27
16	*p*-Xylene	0.4	24	-	-	64	2	15	15	4

[a] Reaction conditions: catalyst 0.1 g, substrate/N_2/H_2 = 1/26/78, ambient pressure, 533 K. *p*-Xy = *p*-xylene, EB = ethylbenzene, T = toluene, B = benzene, Hy = products with cyclohexane ring, Others = C2-C5 hydrocarbons. [b] Selectivity to ethane.

Table 2. Summary of characterization data

Catalyst	BET surface area [$m^2\ g^{-1}$]	d_{XRD} [nm]	d_{TEM} [nm]	Chemisorption H/Ru	Catalytic reaction[e]	
					Conv. [%]	Select. [%][f]
$Ru(4)/CeO_2^{873}$	84	-[a]	-[c]	0.89	95	69
$Ru(1)/CeO_2^{873}$	85	-[a]	-[c]	1.0	27	66
$Ru(0.5)/CeO_2^{873}$	83	-[a]	-[c]	0.56	19	18
$Ru(4)/CeO_2^{1073}$	42	-[a]	1.8	0.72	79	62
$Ru(1)/CeO_2^{1073}$	40	-[a]	1.1	0.71	22	22
$Ru(0.5)/CeO_2^{1073}$	39	-[a]	-[d]	0.56	14	13
$Ru(4)/ZrO_2^{973}$	44	6.0	7.7	0.19	20	62
$Ru(4)/MgO^{973}$	146	15	>10	0.03	18	68
$Ru(4)/TiO_2^{973}$	44	-[b]	4.3	0.29	14	67
$Ru(4)/SiO_2^{973}$	435	3.6	4.5	0.27	10	65
$Ru(4)/Al_2O_3^{973}$	116	6.9	7.9	0.35	4	59

[a] XRD peaks for Ru metal were too small to observe. [b] XRD peaks for Ru metal were overlapped with support peaks. [c] Difficult to determine because of the low contrast between support and Ru particles. [d] No Ru particles were observed. [e] Data from Figures 2 and 3. $W/F = 0.4\ g_{cat}\ h\ mol^{-1}$. [f] C-based selectivity to toluene.

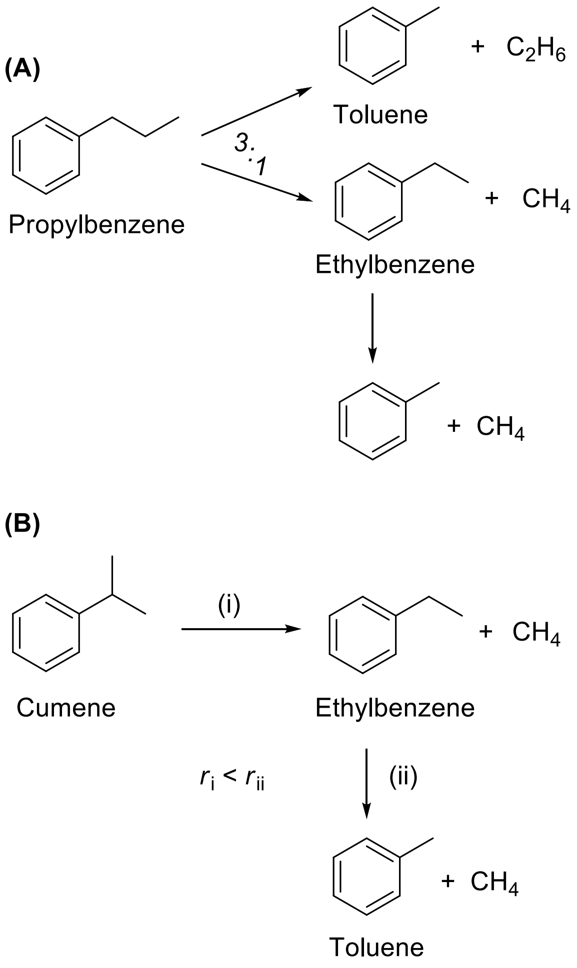

Scheme 1. Reaction route of hydrogenolysis of propylbenzene (A) and cumene (B).

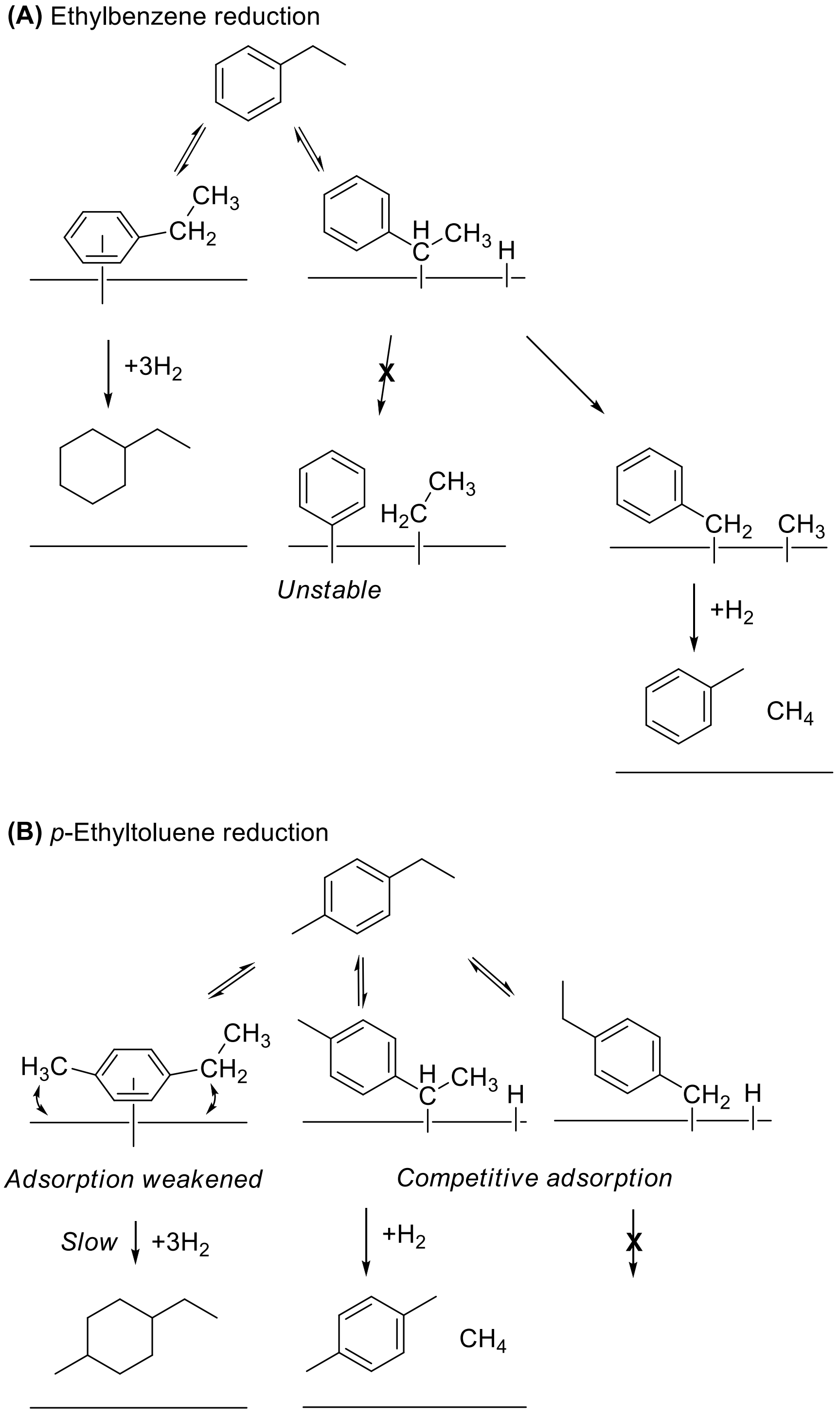

Scheme 2. Reaction mechanisms of ethylbenzene (A) and *p*-ethyltoluene (B) reductions.

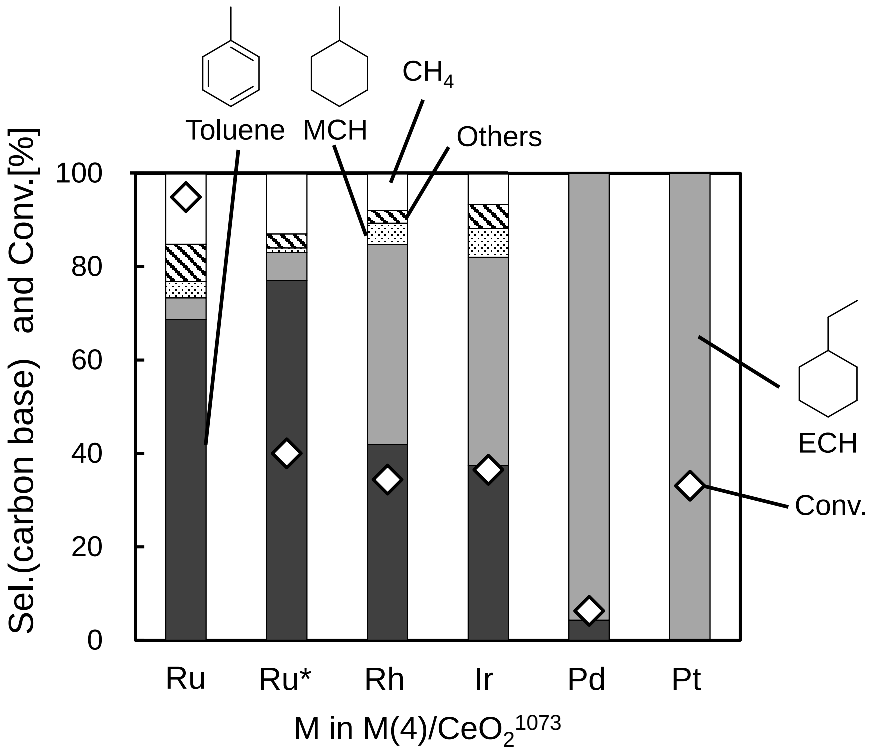

Figure 1. Hydrogenolysis of ethylbenzene over various noble metal/CeO_2 catalysts. Reaction conditions: catalyst 0.1 g, *W*/*F* = 0.4 g_{cat} h mol^{-1} (*: 0.1 g_{cat} h mol^{-1}), ethylbenzene/N_2/H_2 = 1/26/78, 533 K. Others = C2-C6 hydrocarbons.

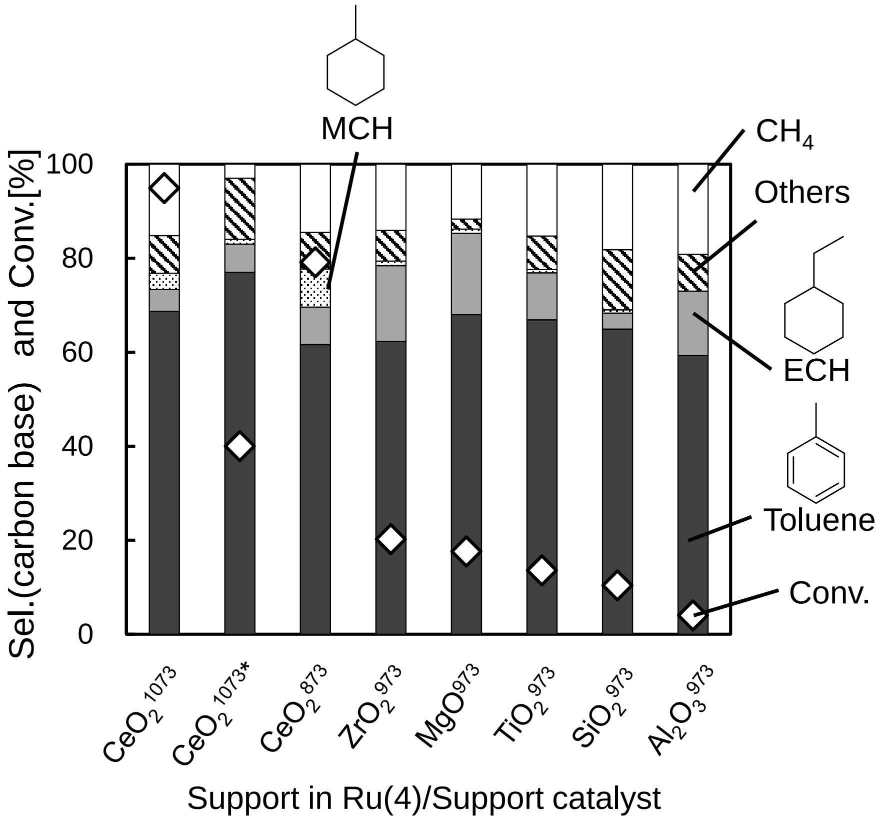

Figure 2. Hydrogenolysis of ethylbenzene over Ru/Support catalysts. Reaction conditions: catalyst 0.1 g, *W*/*F* = 0.4 g_{cat} h mol^{-1} (*: 0.1 g_{cat} h mol^{-1}), ethylbenzene/N_2/H_2 = 1/26/78, 533 K. Others = C2-C6 hydrocarbons.

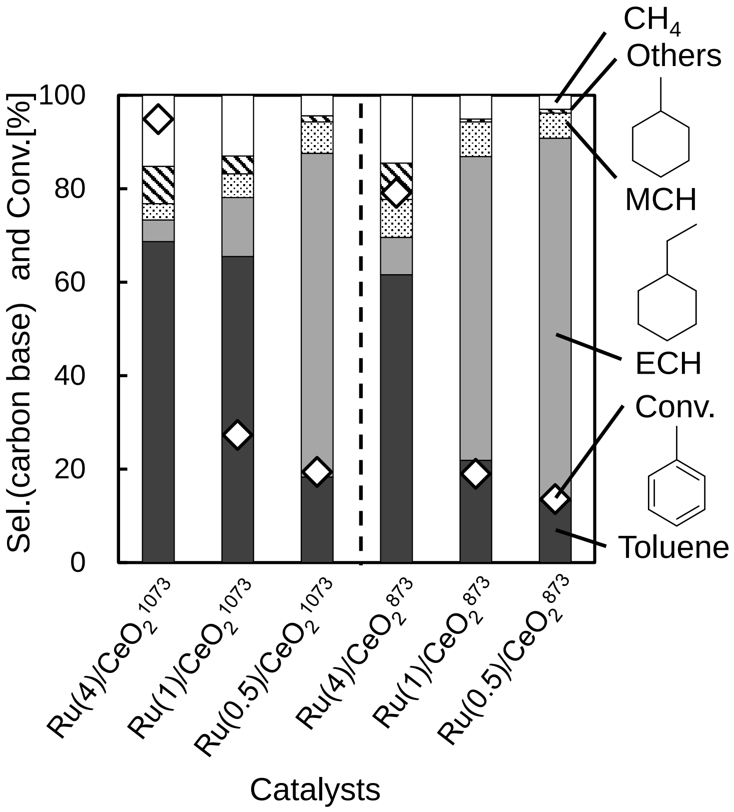

Figure 3. Hydrogenolysis of ethylbenzene over various Ru/CeO_2 catalysts with different Ru loading amount and pre-calcination temperature for CeO_2 support. Reaction conditions: catalyst 0.1 g, *W*/*F* = 0.4 g_{cat} h mol^{-1}, ethylbenzene/N_2/H_2 = 1/26/78, 533 K. Others = C2-C6 hydrocarbons.

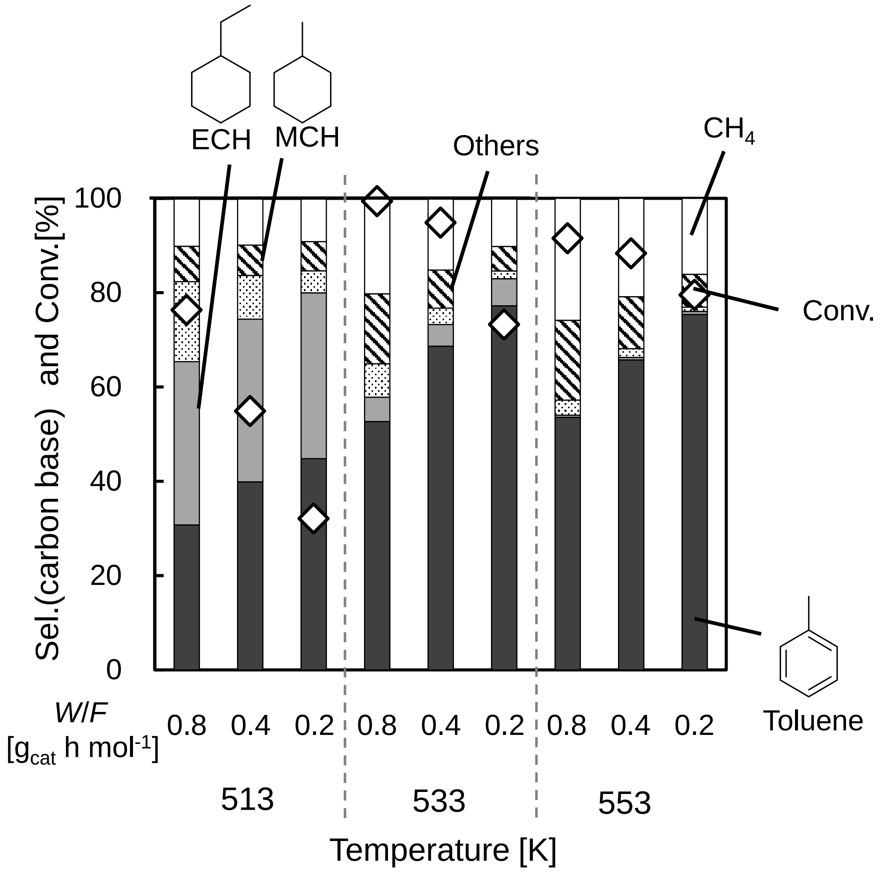

Figure 4. Effect of reaction temperature on hydrogenolysis of ethylbenzene over Ru(4)/CeO_2^{1073}. Reaction conditions: catalyst 0.1 g, ethylbenzene/N_2/H_2 = 1/26/78, ambient pressure. Others = C2-C6 hydrocarbons.

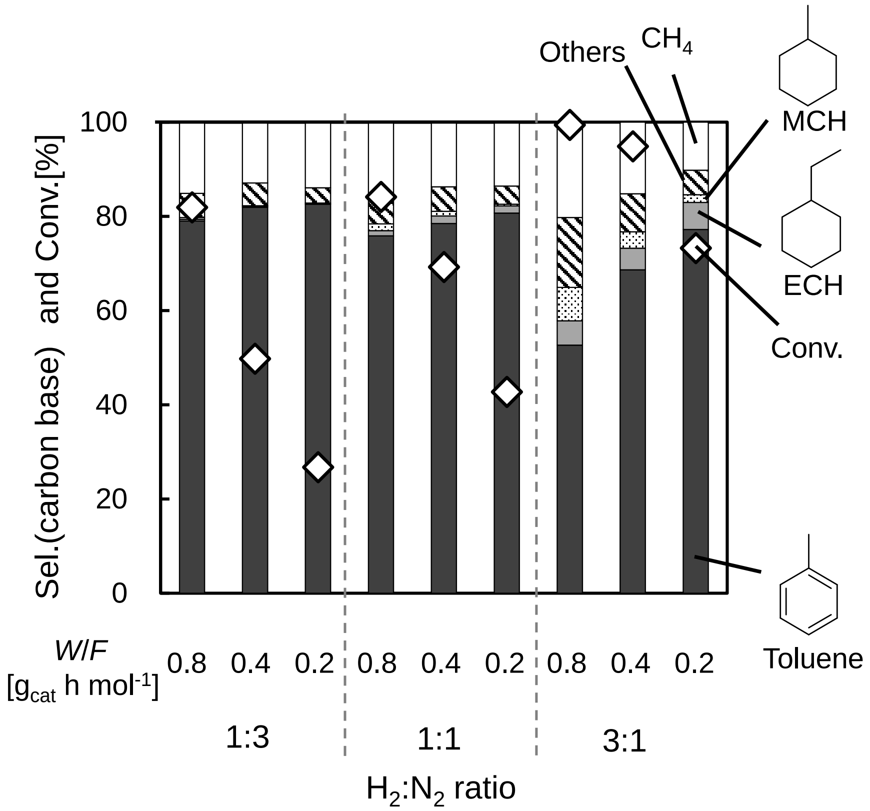

Figure 5. Effect of H_2 pressure on hydrogenolysis of ethylbenzene over Ru(4)/CeO_2^{1073}. Reaction conditions: catalyst 0.1 g, ethylbenzene/(N_2+H_2) = 1/104, ambient pressure. Others = C2-C6 hydrocarbons.

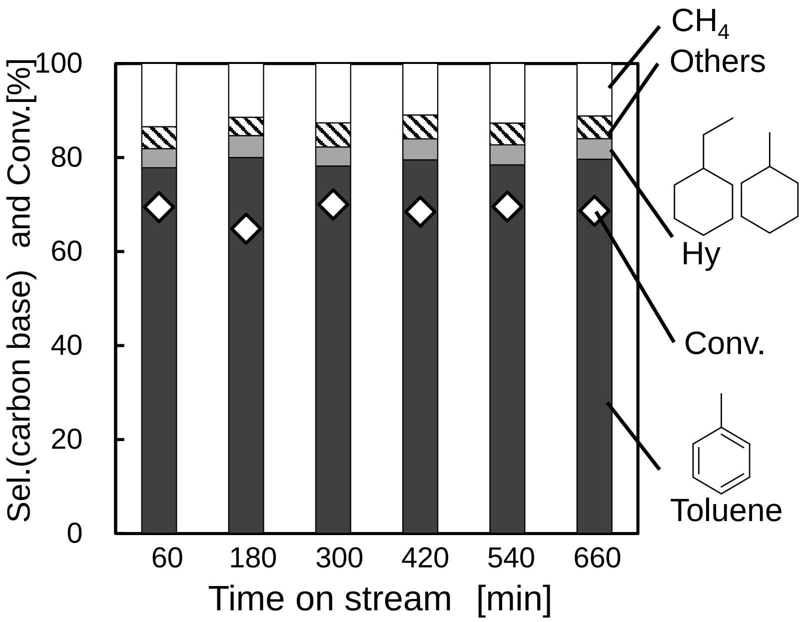

Figure 6. Stability test of Ru(4)/CeO_2^{1073} for hydrogenolysis of ethylbenzene. Reaction conditions: catalyst 0.1 g, *W*/*F* = 0.2 g_{cat} h mol^{-1}, ethylbenzene/N_2/H_2 = 1/26/78, 533 K. Hy = products with cyclohexane ring.

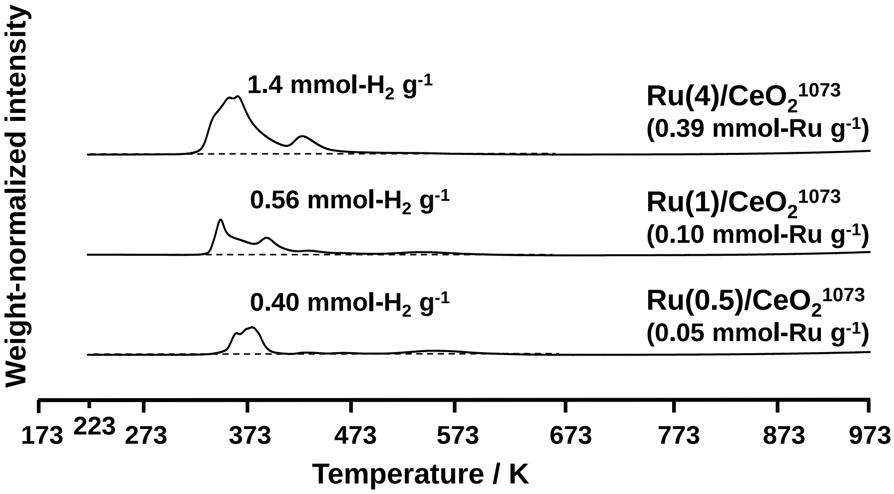

Figure 7. H_2-TPR profiles of Ru/CeO_2^{1073} catalysts. Measurement conditions: H_2/Ar (5% v/v, 30 mL min^{-1}), heating rate 10 K/min, from 223 K to 973 K.

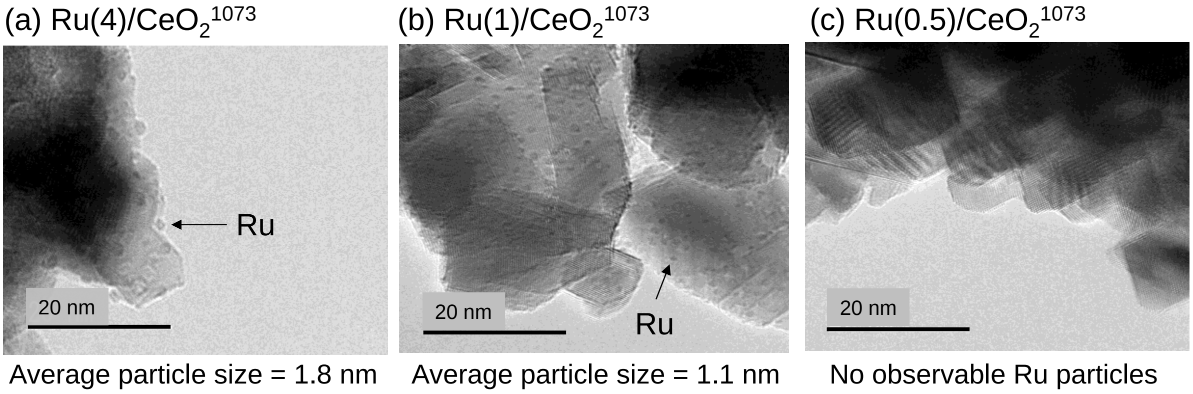

Figure 8. TEM images of Ru/CeO$_2^{1073}$ catalysts after reduction with H_2 at 533 K.

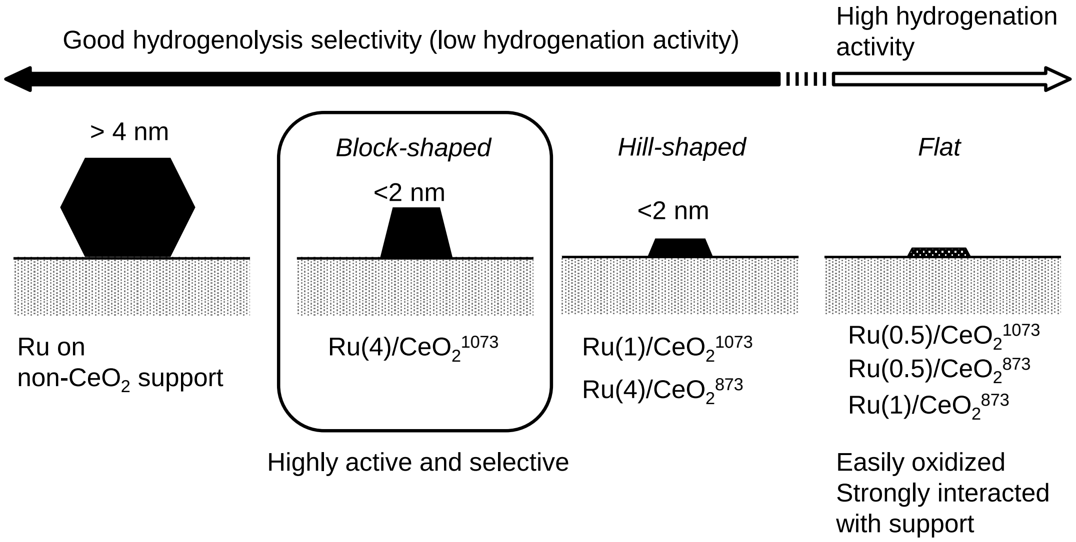

Figure 9. Schematic representation of the structure of Ru catalysts and the performance.

Graphical abstract

FULL PAPER

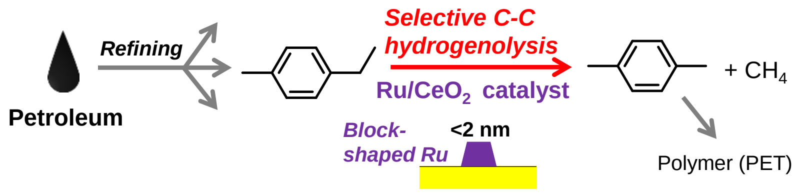

Trimming side chains: Precise control of reaction conditions and structure of Ru/CeO2 catalyst enables convert long alkyl chains of alkylbenzenes into methyl groups by selective hydrogenolysis with suppression of ring hydrogenation.

Shin Yanatake, Yosuke Nakaji, Mii Betchaku, Yoshinao Nakagawa, Masazumi Tamura, Keiichi Tomishige**

Page No. – Page No.

Selective C-C Hydrogenolysis of Alkylbenzenes to Methylbenzenes with Suppression of Ring Hydrogenation